LA-UR-25-20071

Approved for public release; distribution is unlimited.

Title: Godiva IV Simulated Radiation Field Characterization and Variance Reduction

Author(s): Simeonov, Pavel Georgiev
Weldon, Robert Allen Jr.
Whitman, Nicholas Hunter

Intended for: Report

Issued: 2025-01-10 (rev.1)

Godiva IV Simulated Radiation Field Characterization and Variance Reduction

2024 Summer Report

P.G. Simeonov, R.A. Weldon Jr., N.H. Whitman

LA-UR-25-20071
July 26, 2024

Los Alamos
NATIONAL LABORATORY

Contents

Figures

1 Introduction

Godiva IV is a system comprised of highly enriched uranium alloyed with molybdenum in the form of fuel plate rings [3]. The reactor, along with its predecessors, was designed with the unique ability to satisfy interests in the super-prompt-critical reactor operation space. Originally, the reactor was part of the Los Alamos Critical Experiments Facility (LACEF) at Technical Area-18 (TA-18). The radiation field around Godiva at this facility was well characterized and understood. As a fast neutron system, the neutron spectrum in and around Godiva was close to a Watt Fission spectrum. The Kiva where Godiva IV was located at LACEF was made of thin, sheet metal walls which did not contribute significantly to the neutron spectrum.

Following the transition of LACEF to the National Critical Experiments and Research Center (NCERC) in Nevada, Godiva-IV was moved from TA-18 to the Device Assembly Facility (DAF) at the Nevada National Security Site (NNSS). Part of this move brought renewed interest in radiation field characterization. The new facility introduced significant changes to the environment surrounding Godiva, and preliminary foil irradiation results suggested that the room contribution to the neutron spectrum was significant. Unlike at TA-18, a large thermal neutron signature was added to the fast spectrum from Godiva due to significant room return.

A primary goal due to the additional complexity that the room return adds to the Godiva IV radiation emission spectrum was the development of an efficient Monte Carlo N-Particle (MCNP) calculation capable of characterizing the neutron spectrum anywhere in the room around Godiva. A campaign of activation foil irradiations and analysis were completed to support the validation of the MCNP model. The modeling of these foils in MCNP can be easily done with a standard volumetric neutron flux tally. However, given the multitude of locations and reaction rates to be modeled, further steps must be taken to increase the efficiency of these calculations in MCNP.

During this study, a benchmark model currently under development for Godiva IV [2] was used. A qualitative assessment of the thermal neutron contributors was performed using spatial neutron distribution plots. Additional detail was added to the model based on the qualitative results showing the thermal spectrum's large sensitivity to hydrogenous material. Neutron energy spectra was evaluated at discrete locations in the room around Godiva to quantify the relative contribution of various components. It was discovered that the concrete walls are the largest contributor to the thermal signature, with minor contributions from plastic components surrounding Godiva. Following these results, two different variance reduction techniques were implemented to improve the problem efficiency in these calculations. In the first approach, an F5 point detector tally was implemented in the standard Godiva IV criticality problem. The second approach involved a weight-window generator implementation with an F5 point detector tally in a fixed source problem. The weight window implementation reduced the runtime from 42739.55 minutes to 1803.34 minutes (computer time), compared to the F5 KCODE implementation.

2 Results

2.1 Thermal Neutron Contributors

The contributions to the thermal neutron signature were first evaluated qualitatively using spatial neutron distribution (FMESH) plots. The FMESH plots provided a good visual representation of where significant neutron moderation occurs, and insight to materials and components of interest to the study. Based on the qualitative results, additional components and geometries were added to the Godiva MCNP model to improve the accuracy of calculated spectra. Neutron flux spectrum tallies were then evaluated to quantify the impact of the individual components in the model.

2.1.1 Spatial Neutron Distribution in the Godiva Assembly and Structure

An 100 by 100 centimeter FMESH was evaluated using the benchmark Godiva-IV MCNP benchmark model (Figure 1). The FMESH cells are uniformly distributed across the volume. Two energy bins were specified; a thermal bin for neutrons with energies less than 1 keV, and a fast bin for neutrons with energies greater than 1 keV. The tally was collected over 20,000 KCODE cycles with 10,000 neutrons simulated per cycle.

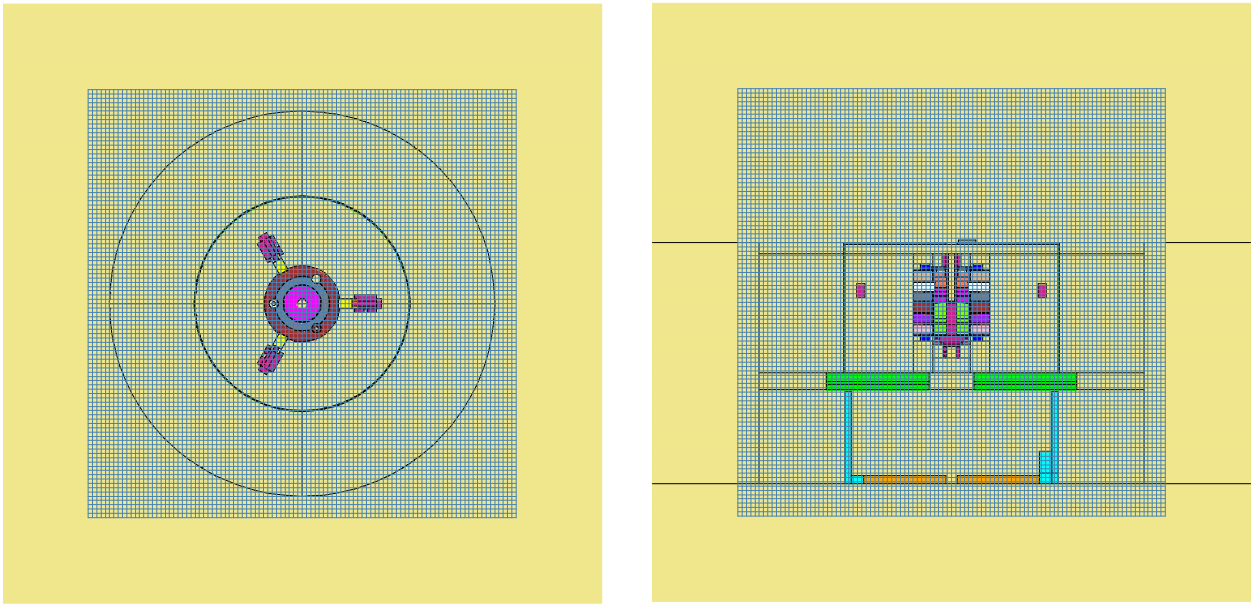

(a) XY Plane at origin

(b) YZ Plane at origin

Figure 1: 100 by 100 cm FMESH Grid

In Figure 2, the FMESH results from the thermal energy bin are plotted in the YZ plane and the XY plane. The acrylic contamination box under the Godiva assembly has a significant contribution to the total neutron thermalization based on these views. These observations informed the next additions to the model. Any hydrogenous material near Godiva or with a large volume in the room was expected to have a significant contribution to the thermal neutron spectrum. In Figure 3, the same plots were created but for the fast energy neutron bin results. These results confirmed expectations for neutron shadowing from the steel and other structural elements.

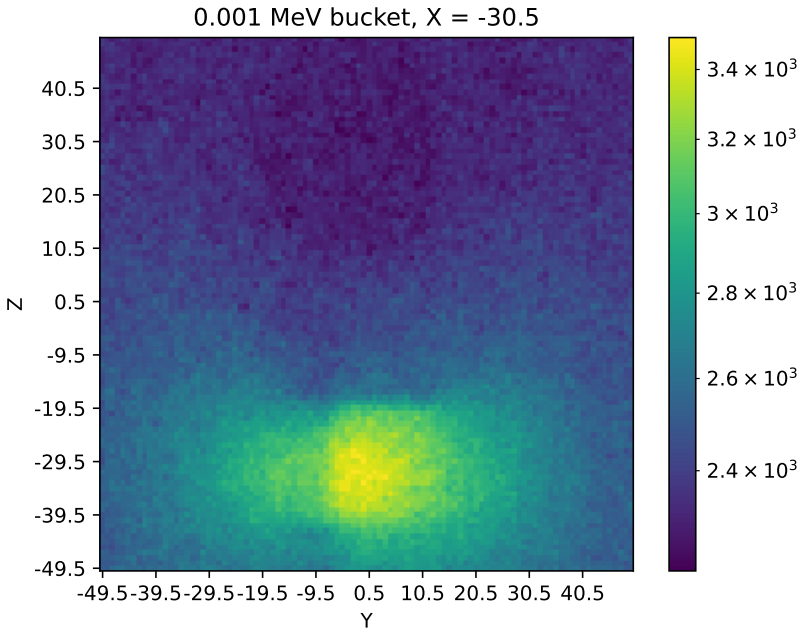

(a) YZ Plane vs. X

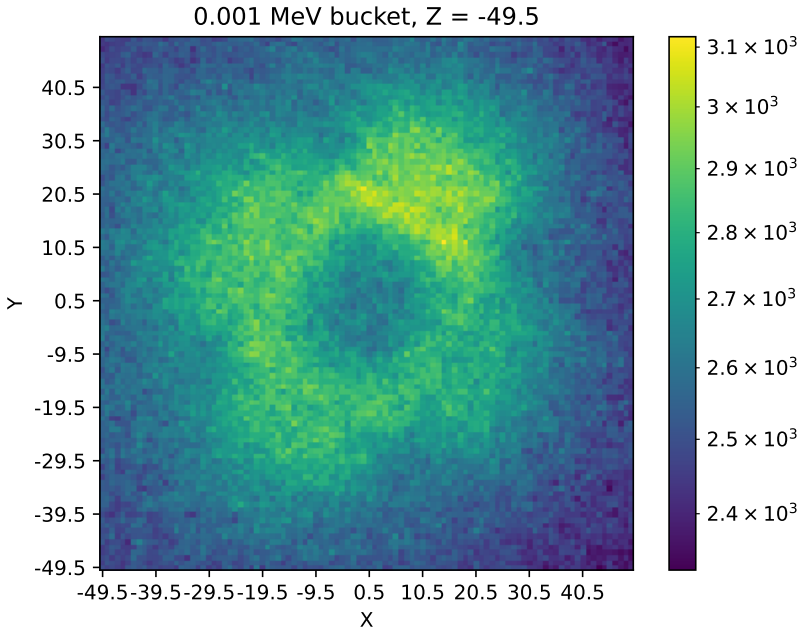

(b) XY Plane vs. Z

Figure 2: 100 by 100 cm FMESH Results, Relative Thermal Neutron Flux

Note: This figure is an animated GIF. Please use a compatible PDF viewer to see the intended video.

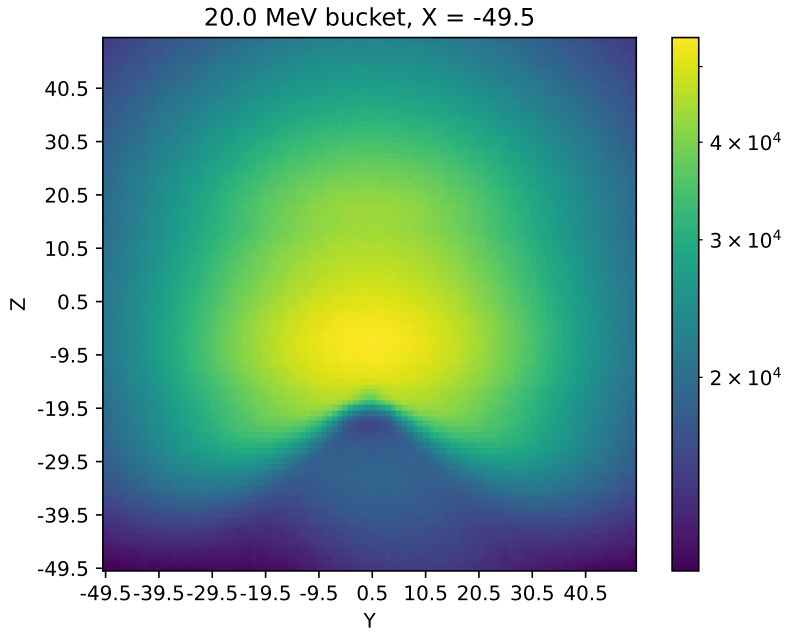

(a) YZ Plane vs. X

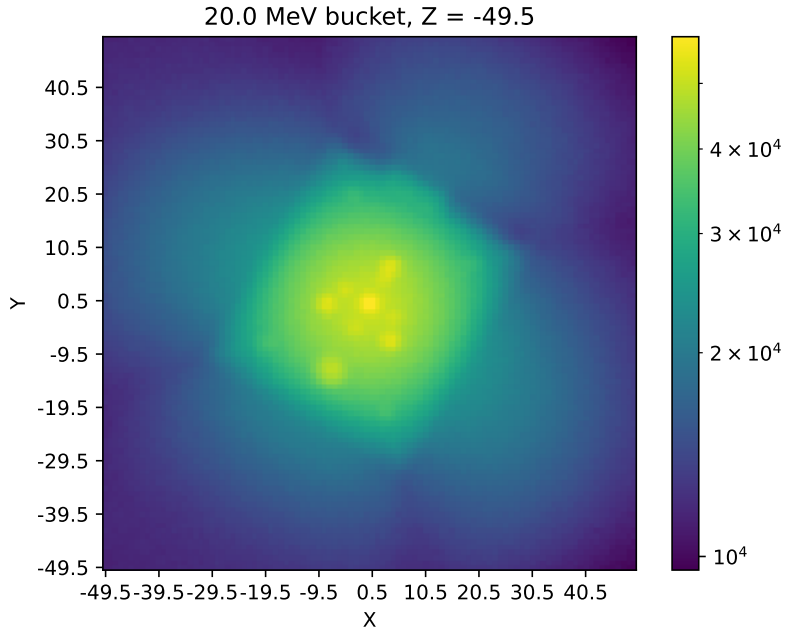

(b) XY Plane vs. Z

Figure 3: 100 by 100 cm FMESH Results, Relative Fast Neutron Flux

Note: This figure is an animated GIF. Please use a compatible PDF viewer to see the intended video.

2.1.2 Godiva Model Modifications

Informed by the FMESH plots, hydrogenous components missing from the model were added to improve the accuracy of calculated spectra. The plastic scintillator detectors adjacent to the Godiva core, visible in Figure 4a and 4d as tan/magenta cylinders, were added.

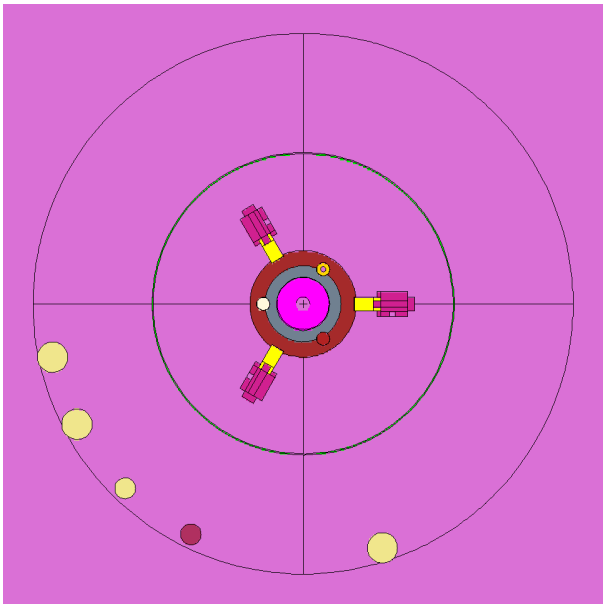

(a) XY view at origin

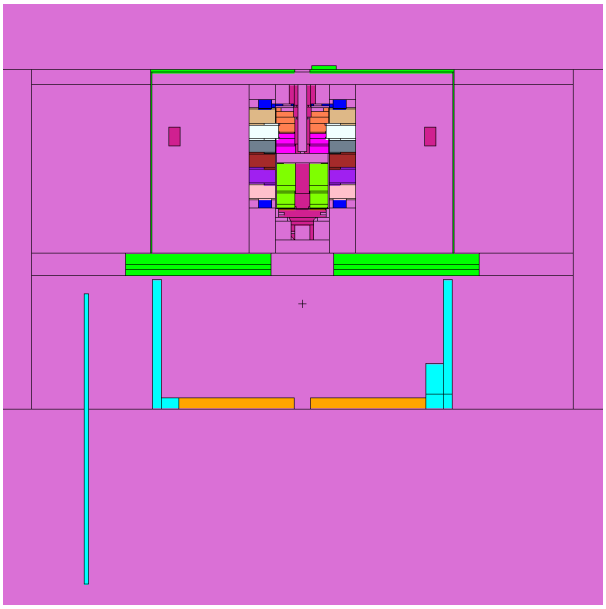

(b) YZ view at origin

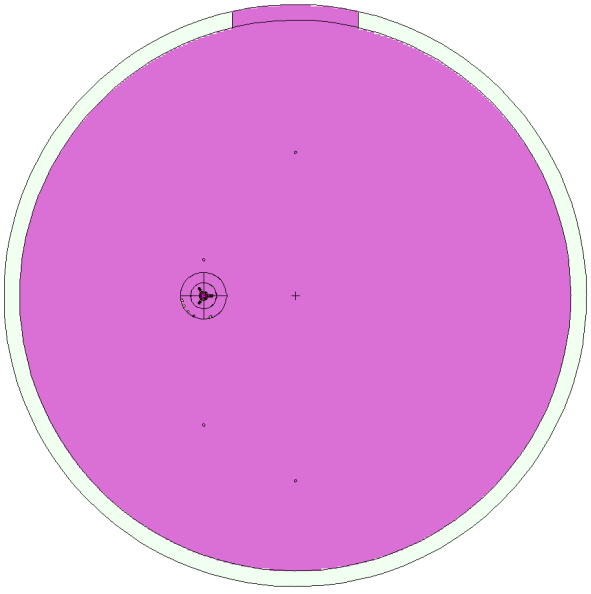

(c) XY view at origin, full geometry

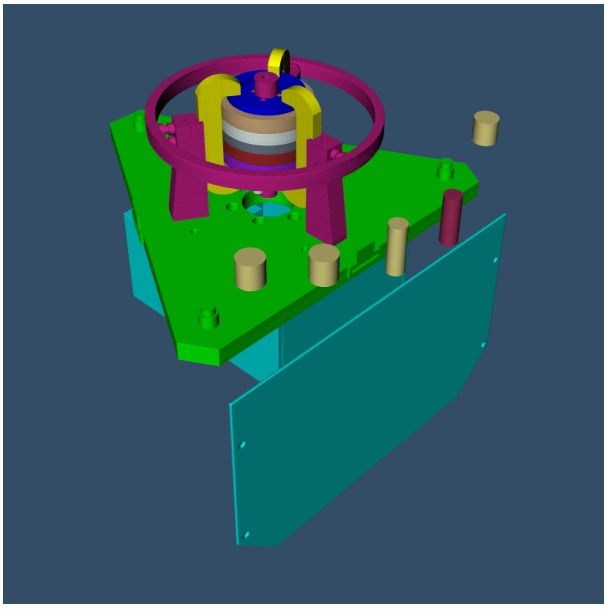

(d) Isometric view

Figure 4: Godiva MCNP Model Modifications

Out of the three middle detectors, the two on the left are EJ204 (PVT) scintillator detectors manufactured by Eljen Technology. The third is a LYSO scintillator detector manufactured by Berkeley Nucleonics Corporation. In the model, material composition of PVT and LYSO assumed literature values [1]. The two detectors on either side of the middle three detectors are part of the Godiva reactor control system. The model approximated these two detectors as equivalent sized EJ204 detectors. The next item that was added to the model is the acrylic shield below those detectors, shown in Figure 4d as a light blue plate, meant to provide a barrier between the detector cables and the Godiva IV mechanical actuators. Lastly, the room entrance was modeled explicitly (top of Figure 4c).

2.1.3 Spatial Neutron Distribution in the Full Room

A second FMESH tally was run with the modifications. The FMESH was modified to capture the entire Godiva room, which covers an approximate 1000 by 1000 by 500 centimeter rectangular volume. Each spatial cell of the FMESH was set to 5 centimeters, instead of 1. Three energy bins were specified with cutoffs at 1 eV, 10 keV, and 100 MeV, for thermal, epithermal, and fast energy regions respectively. The results of the FMESH tally was plotted in the XY plane for every Z value and compiled in Figures 5-7 for the thermal, epithermal, and fast energy bins respectively.

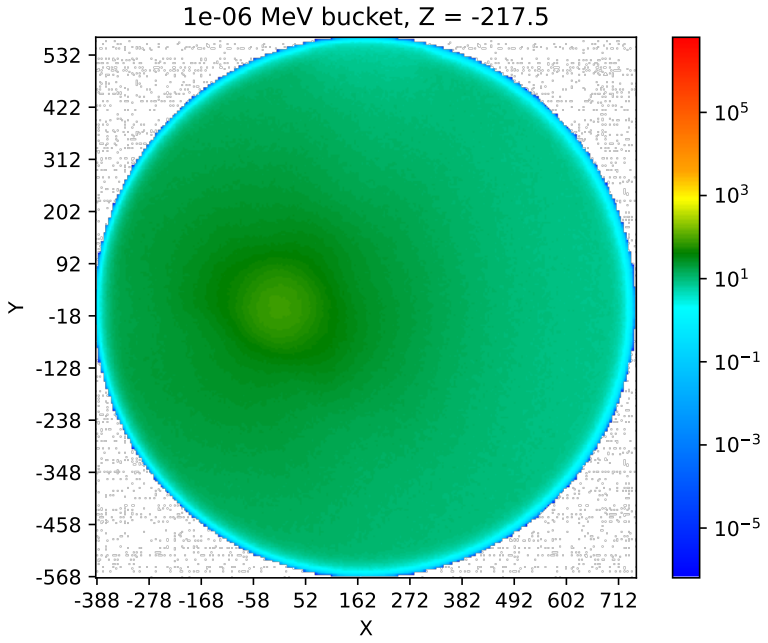

Figure 5: 1000 by 1000 cm FMESH, Relative Thermal Neutron Flux

Note: This figure is an animated GIF. Please use a compatible PDF viewer to see the intended video.

These results identified the significance of the thick concrete wall, floor, and ceiling. The absence of concrete in the room entrance also has a visible effect on the spectrum near the entrance. The plastic detectors south of Godiva and the plastic contamination box under Godiva are observed to have a large impact to the epithermal neutron flux, rather than the thermal neutron flux.

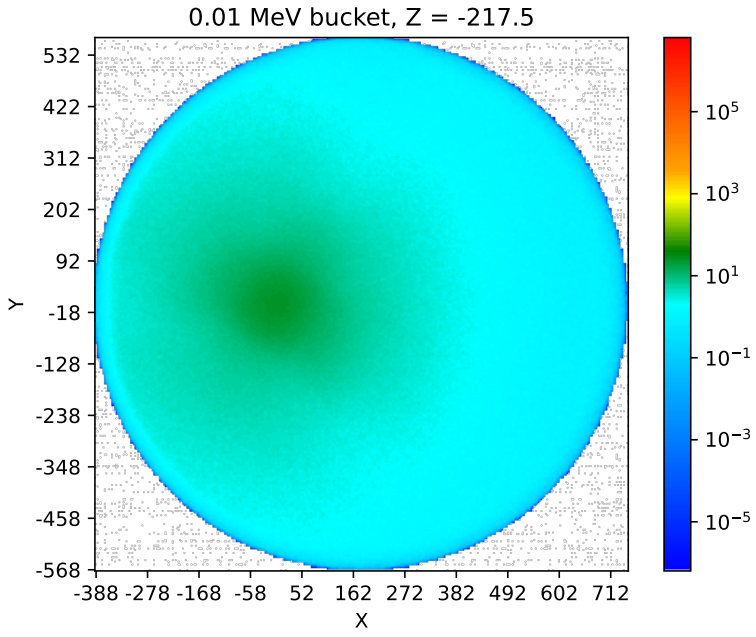

Figure 6: 1000 by 1000 cm FMESH, Relative Epithermal Neutron Flux

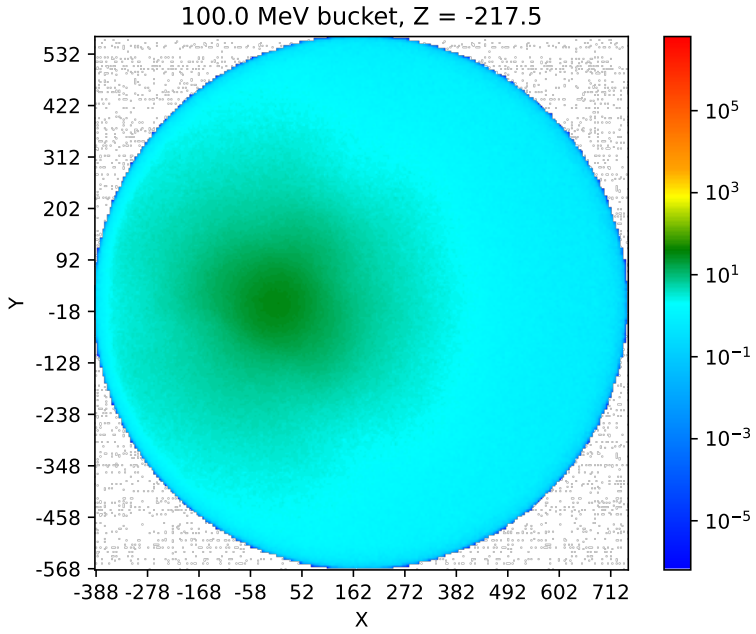

Figure 7: 1000 by 1000 cm FMESH, Relative Fast Neutron Flux

Note: This figure is an animated GIF. Please use a compatible PDF viewer to see the intended video.

These results identified the significance of the thick concrete wall, floor, and ceiling. The absence of concrete in the room entrance also has a visible effect on the spectrum near the entrance. The plastic detectors south of Godiva and the plastic contamination box under Godiva are observed to have a large impact to the epithermal neutron flux, rather than the thermal neutron flux. Lastly, in the fast energy plot the neutron shadowing from the structural elements of the assembly is observed to extend across the entire room.

2.1.4 Neutron Energy Spectrum at Discrete Locations

Both FMESH simulations provided qualitative representations of the effects of materials of interest in the room. A numerical comparison of contributions from the materials was also desired. The neutron flux was tallied at four discrete distances (0.7, 2.5, 3.3, and 4.0 meters) away from Godiva with an F4 volumetric neutron flux tally in the KCODE model. The cells chosen for the tally are spheres with a 2.5 centimeter radius. The energy bins selected were distributed evenly on the logscale from 1e-9 to 20 MeV to capture the entire energy distribution in great detail. The KCODE parameters were set to simulate 1e6 neutrons for 6e4 cycles. Four separate cases were simulated:

1. Full Godiva-IV model, including the entire room, room entrance, scintillator detectors, and plastic shield

2. Full Godiva-IV model with modification replacing all plastic with air

3. Full Godiva-IV model with modification replacing all plastic and concrete with air

4. Full Godiva-IV model with modification replacing all concrete with air

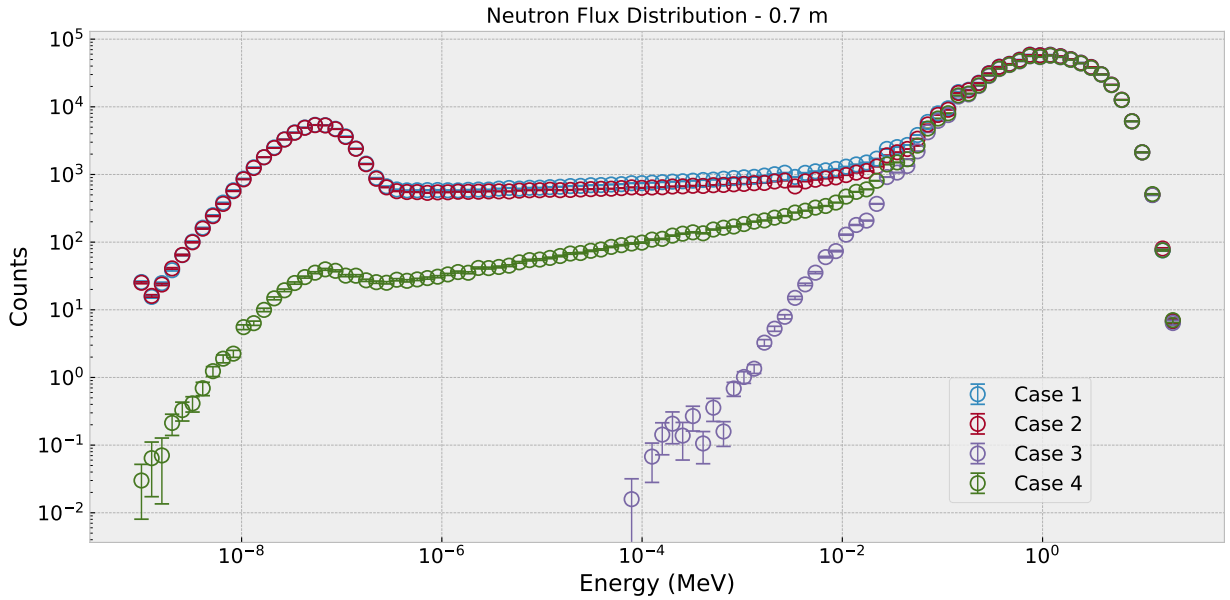

Figure 8: Neutron Energy Distribution at 0.7 meters from Godiva

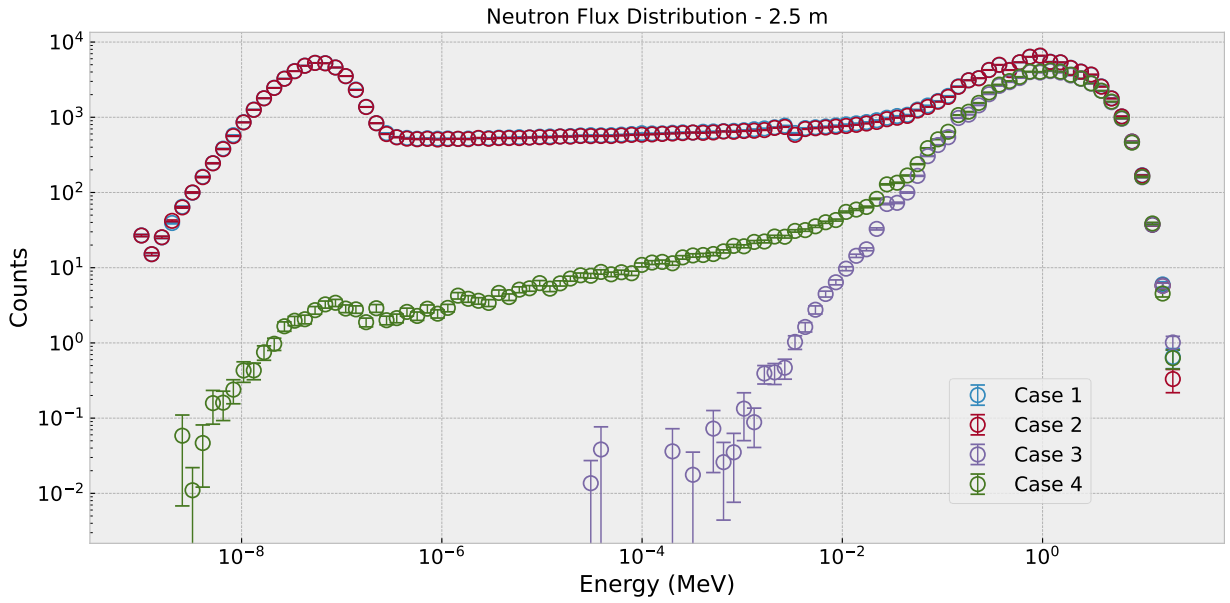

Figure 9: Neutron Energy Distribution at 2.5 meters from Godiva

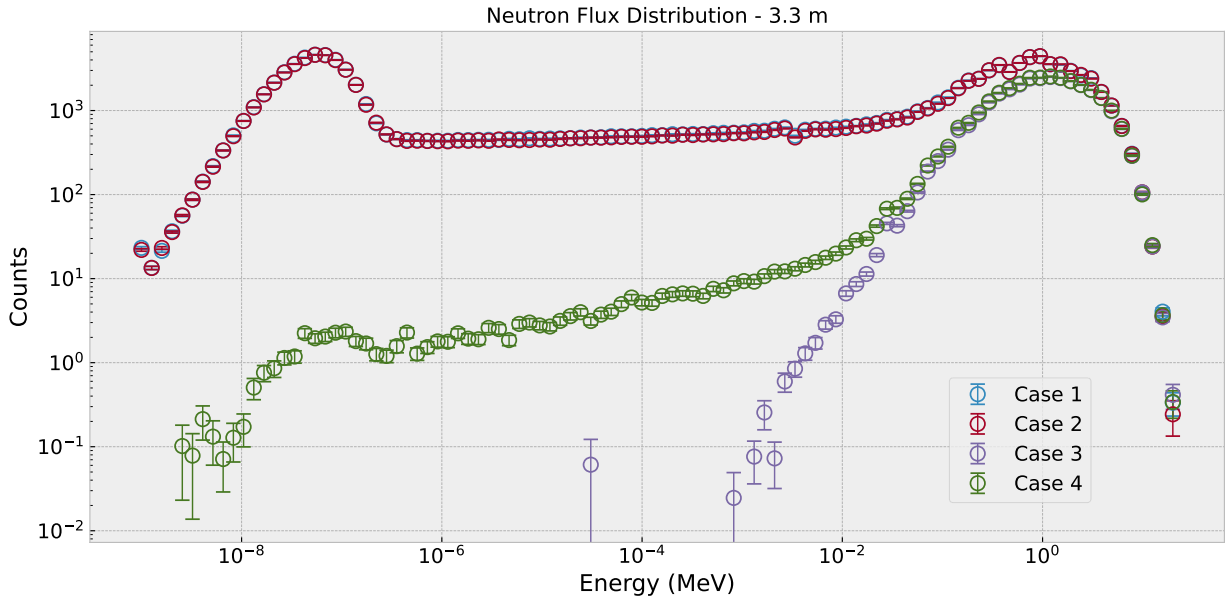

Figure 10: Neutron Energy Distribution at 3.3 meters from Godiva

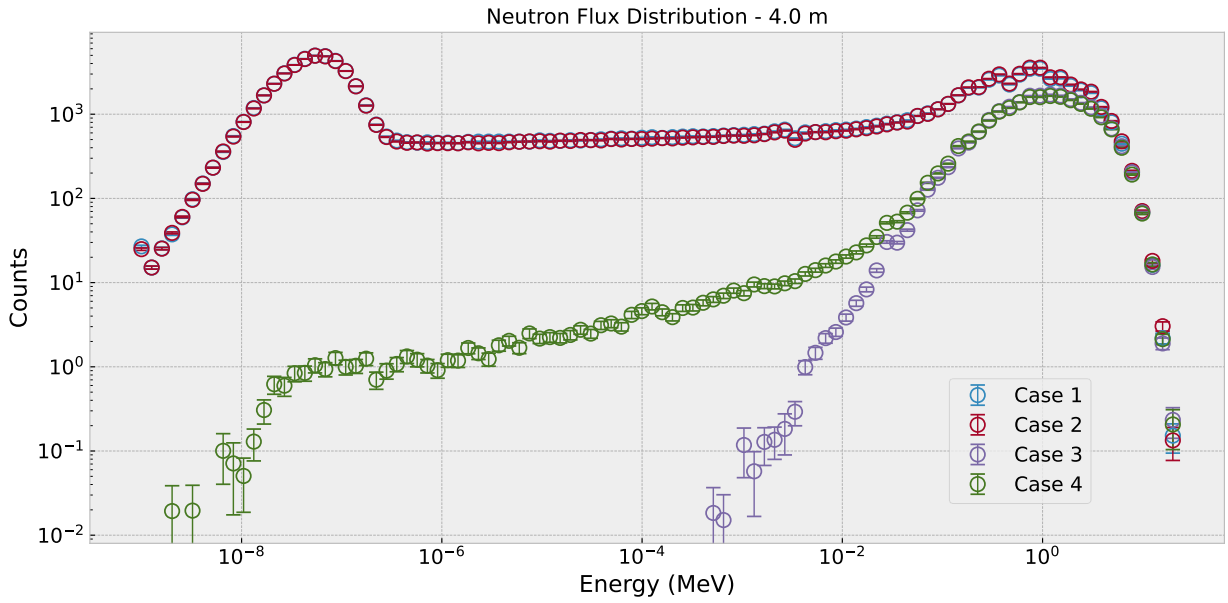

Figure 11: Neutron Energy Distribution at 4.0 meters from Godiva

These results (Figures 8-11) provided insight to the relative contributions of the hydrogenous materials in the room. In Figure 8, the contribution of the plastic to the epithermal neutron flux region is visible. At all locations, the concrete is confirmed to be the major source of thermal neutrons. In the absence of the concrete and plastic (Case 3) the neutron energy distribution is an entirely fast spectrum, providing further verification that the major contributors are concrete and plastic. In Figure 8, the fast energy peak at 0.7 meters is approximately an entire order of magnitude larger than the thermal energy peak. In comparison, the further locations at 2.5, 3.3, and 4.0 meters show that the fast energy peak reduces as a function of distance while the thermal peak remains the same magnitude. In Figure 11, the thermal energy peak for the 4.0 meter location is greater than the fast energy peak.

2.2 Variance Reduction Technique Implementation and Verification

A desired capability for dosimetry modeling in the room with Godiva is quick turnaround time for tally reaction rates. A couple of different techniques were investigated to determine their effectiveness and applicability to the Godiva MCNP problem. For both techniques, the neutron spectrum obtained at the four target locations with the F4 volumetric neutron flux tally was used for verification.

In MCNP, tally variance is inversely proportional to particles simulated and simulation runtime, as discussed in Section 1.2.5 of the MCNP 6.3 manual [4]. There are games that can be played to bias the simulation in favor of particles that add to a desired tally. This appears to harm the physics of the simulation, however, advanced variance reduction techniques in MCNP account for this bias and provide the correct answer while reducing the computational expense when applied appropriately.

2.2.1 F5 Point Detector Tally

The first variance reduction technique that was tested was the F5 point detector tally with the same KCODE model used for the first case in Figures 8-11. Four F5 tallies were placed at the same Cartesian coordinates as the 2.5 centimeter spherical cells used for the F4 volumetric neutron flux tally. The same energy bins were used as the F4 tallies, distributed evenly on the logscale from 1e-9 to 20 MeV. The simulation was run with KCODE parameters set to simulate 1e5 neutrons for 6e3 cycles. For this comparison, the results from the 4.0 meter location will be used as this tally location is the most computationally expensive to run. Figure 12a compares the neutron energy distribution from the F5 tally in KCODE with the true solution obtained from the F4 tally in KCODE and Figure 12b displays the percent relative difference between the two results.

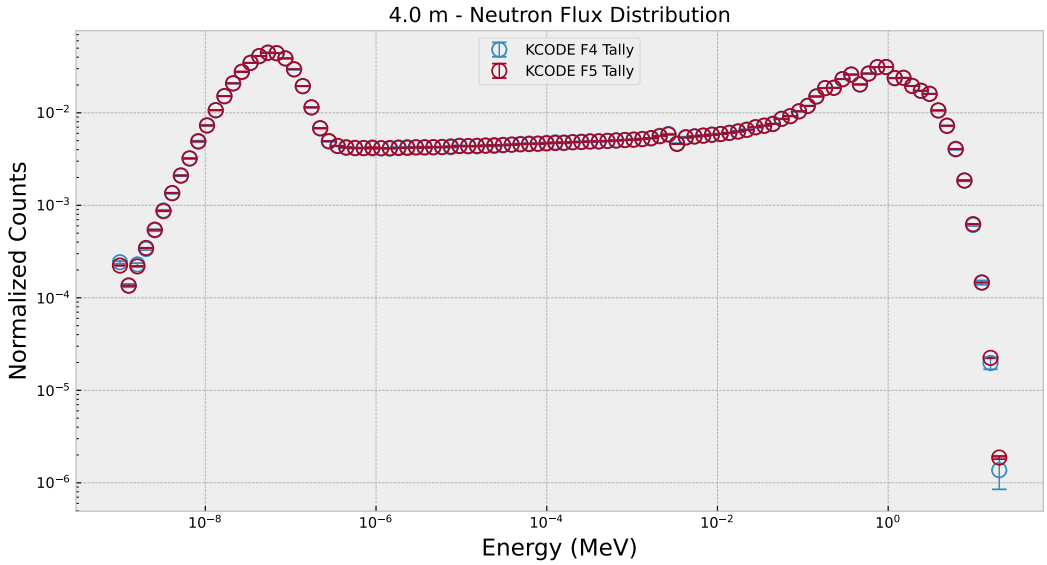

(a) Neutron Energy Distribution

Figure 12: KCODE F4 and F5 Tally at 4.0 meters from Godiva

These results show that the F5 point detector tally achieves a remarkably similar result to the F4 volumetric neutron flux tally while reducing the run-time by an order of magnitude, from 566441.80 minutes to 42739.55 minutes (computer time). Most differences lie within two percent, and all differences are within two standard deviations of zero percent. The large skews in those differences at the lowest and highest ends of the energy distribution have been attributed to the low number of neutrons simulated at those energies.

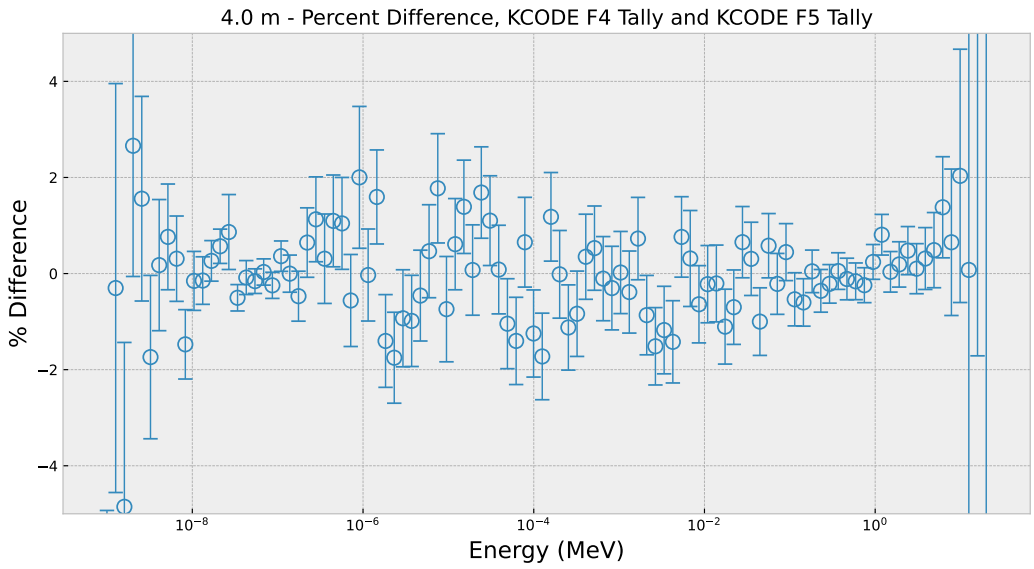

(b) Percent Relative Difference in Neutron Energy Distribution

Figure 12: (Continued) KCODE F4 and F5 Tally at 4.0 meters from Godiva

2.2.2 Godiva Fixed Source Model

The only variance reduction technique that can be run in a KCODE problem is the F5 point detector tally. A source definition for a fixed source problem of the Godiva model was implemented for use in with the other variance reduction technique of interest. Due to the large number of fuel cell cards, the source definition required individually defined sampling volumes for each fuel cell. The source definition was defined to sample spontaneous fission within the fuel cells. To obtain the correct neutron energy spectrum, a high multiplication value for the sub-critical Godiva system was achieved. The neutron energy spectrum for the fixed source model is verified against the existing KCODE results at the 4.0 meter location. The tally cards for both simulations were set to be the same F4 volumetric neutron flux tally from Figure 11. In Figures 13a-13b, a comparison is made similar to the F5 and F4 tally comparison previously discussed.

The results in Figures 13a-13b show similar trends to those discussed previously in the F5 point detector tally spectrum verification. The neutron energy distribution shows good agreement in both visualizations. This confirms that the fixed source problem achieved a neutron energy distribution similar to the original KCODE problem for Godiva.

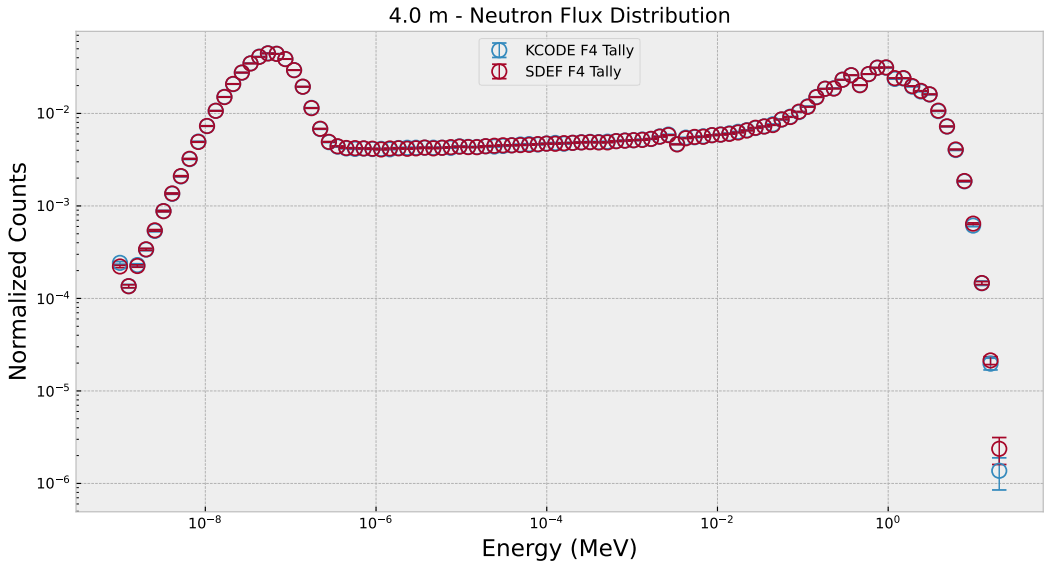

(a) Neutron Energy Distribution

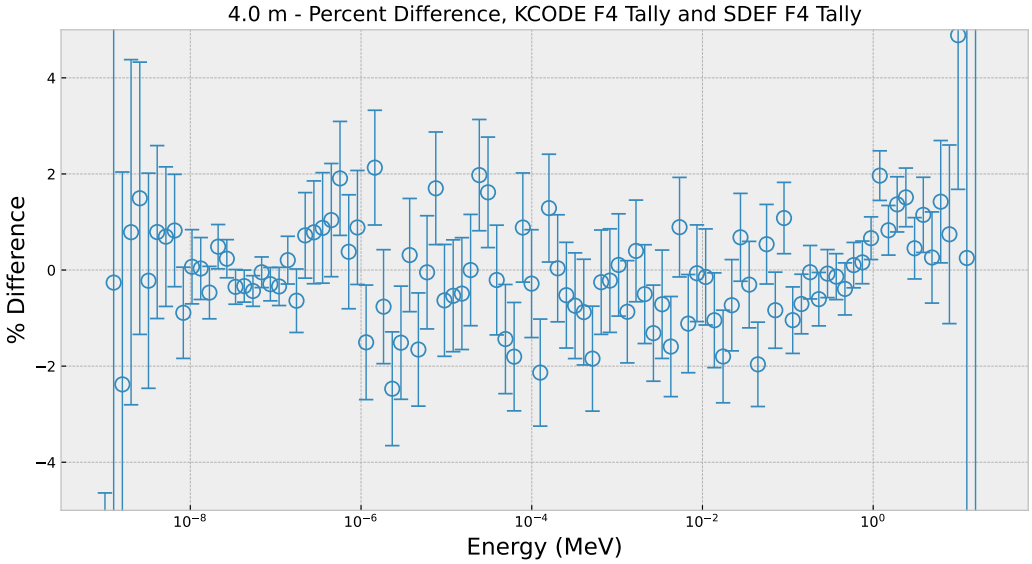

(b) Percent Relative Difference in Neutron Energy Distribution

Figure 13: SDEF F4 and KCODE F4 Tally at 4.0 meters from Godiva

2.2.3 Weight Windows with Point Detector Tallies

The next variance reduction technique tested involved setting weight windows on a F5 point detector tally in the verified fixed source model. Weight windows are an efficient method to control the particle weights in a MCNP simulation for a given target tally. Weight windows work inversely to the importance card; spaces with greater importance are assigned a smaller weight limit. Particles

with a weight larger than the upper weight limit defined are split until the resulting particles have weights within the weight window.

The implementation approach followed general recommendations outlined in the MCNP 6.3 manual. For MCNP models with large spatial domains, it is highly recommended to apply the weight windows on a superimposed mesh over the geometry to appropriately subdivide the domain. Since Godiva is situated in a circular room, a cylindrical mesh was chosen to subdivide the domain (Figure 14). The 4.0 meter tally location, which was the target tally for the weight window, is south of the center of the room in Figure 14. The cylindrical mesh was subdivided into smaller cells in areas of known importance, such as the Godiva assembly, the walls of the room, and the tally.

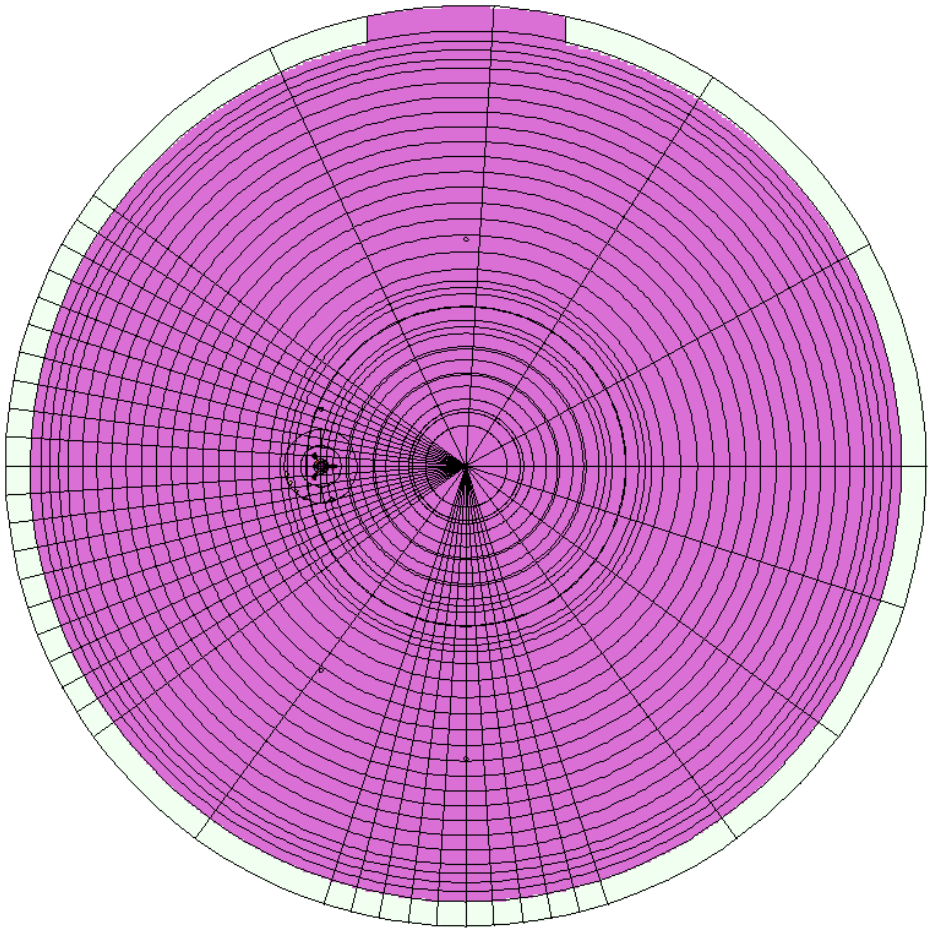

Figure 14: Weight Window Superimposed Mesh for Godiva Model

The weight window generator (WWG) iterative method was used to set the weights for the mesh cells. In the first iteration, the number of source histories was set to 1e7. This is a computationally expensive simulation, but it was determined to be unavoidable as the WWG requires good sampling of the entire domain in order to set appropriate weight windows for the mesh cells. Figure 15 displays the weight window limits that resulted from the first simulation. Figure 15 displays the weight windows produced by the WWG from the first iteration. This process was repeated again, however, the weight windows generated by the first iteration were set as the weight windows for

the second iteration. Figure 16 displays the weight windows produced by the WWG in the second iteration.

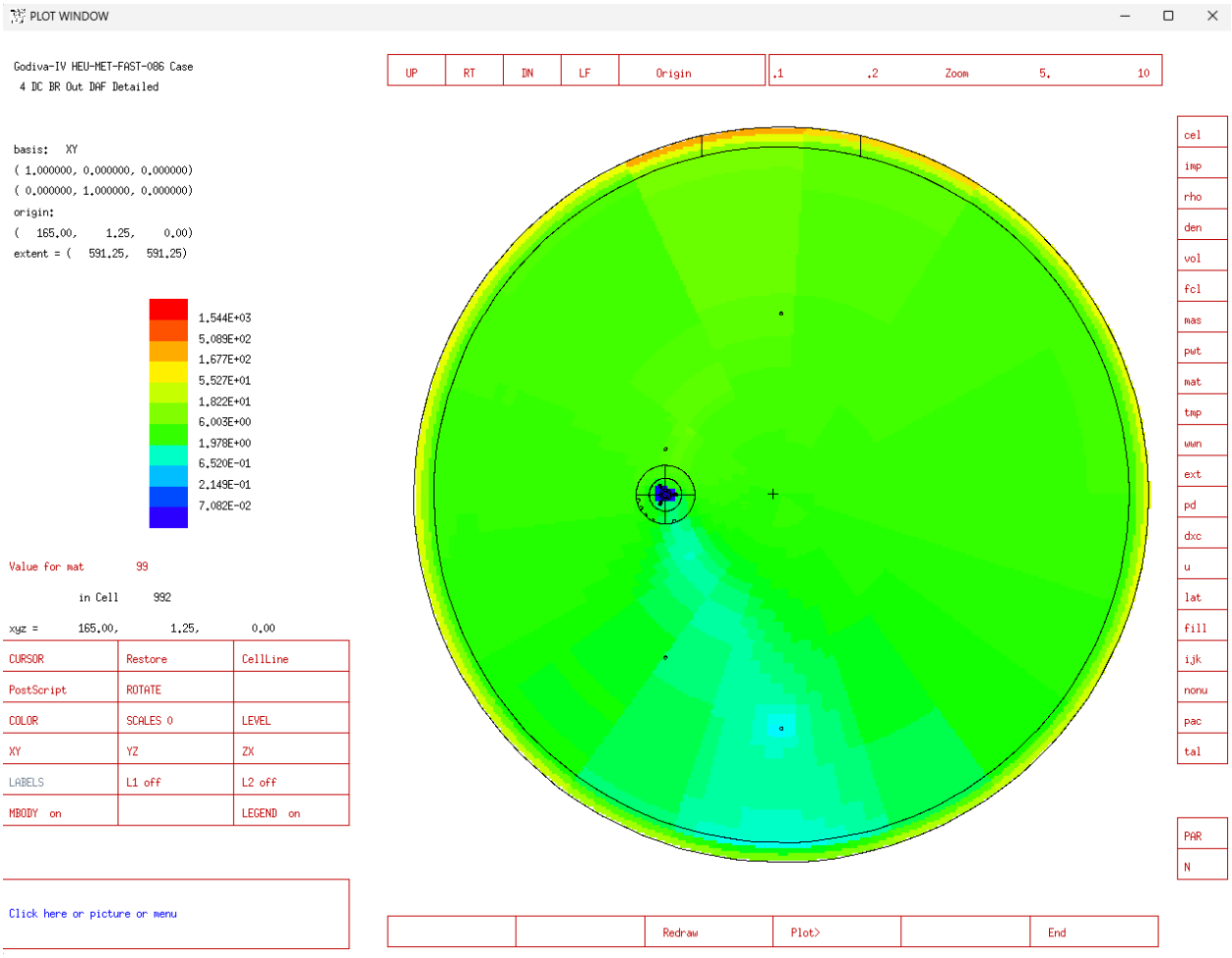

Figure 15: Weight Windows from First Weight Window Generator Iteration

Both weight windows follow the trends that are expected. In Figure 15, the first weight window has set lower weights for the mesh cells around the tally of interest, in the air between the tally and the Godiva assembly, and in the wall directly behind the tally. The weight window also set a high importance to the Godiva assembly itself, which is to be expected. In Figure 16, the second weight window shows improvement over the first by setting a lower weight limit to the aforementioned areas.

An F5 point detector tally simulation was completed with the weight windows set to the WWG output from the second iteration. The tally specifications were set to match those of the F5 tally done before in the KCODE problem. The number of simulated histories in the simulation was set to 1e6. Figure 17 compares the result from the WWG-F5 tally solution with the expected solution obtained from the KCODE F4 tally. Figure 18 displays the percent relative difference between the two results.

The neutron energy spectrum at the 4.0-meter tally location from the F5 tally with weight windows was very similar to the original KCODE F4 tally results. However, this simulation represented

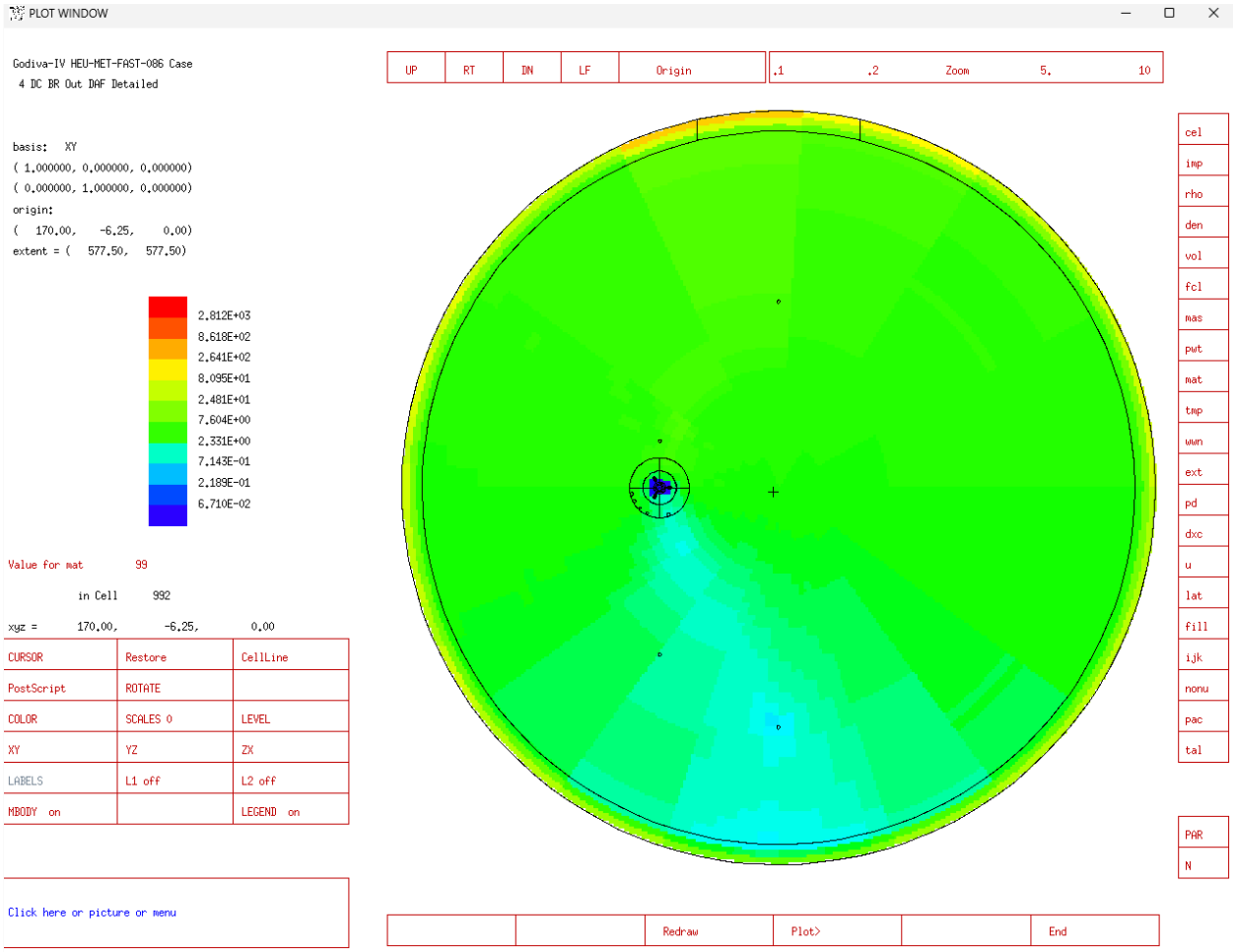

Figure 16: Weight Windows from Second Weight Window Generator Iteration

a further reduction of in runtime compared to the F5 KCODE implementation, from 42739.55 minutes to 1803.34 minutes (computer time). The percent difference for the majority of the energy range falls within two percent, and all differences lie within two standard deviations from zero. The F5 tally was recorded to pass all 10 statistical checks performed by MCNP. These preliminary results show that weight windows can be effective within the room with Godiva.

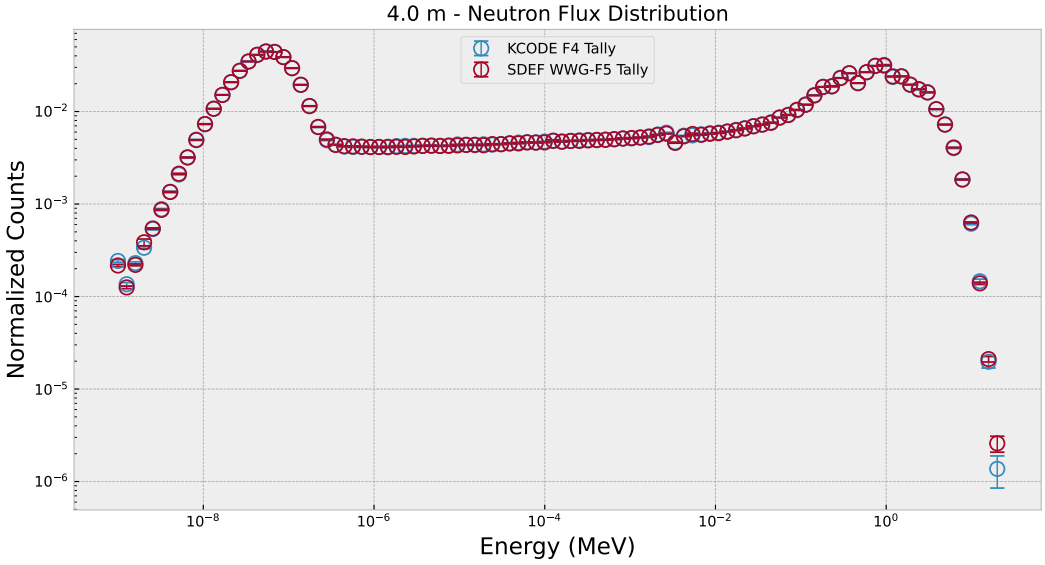

Figure 17: Neutron Energy Distribution at 4.0 meters from Godiva, SDEF F5 tally with Weight Windows

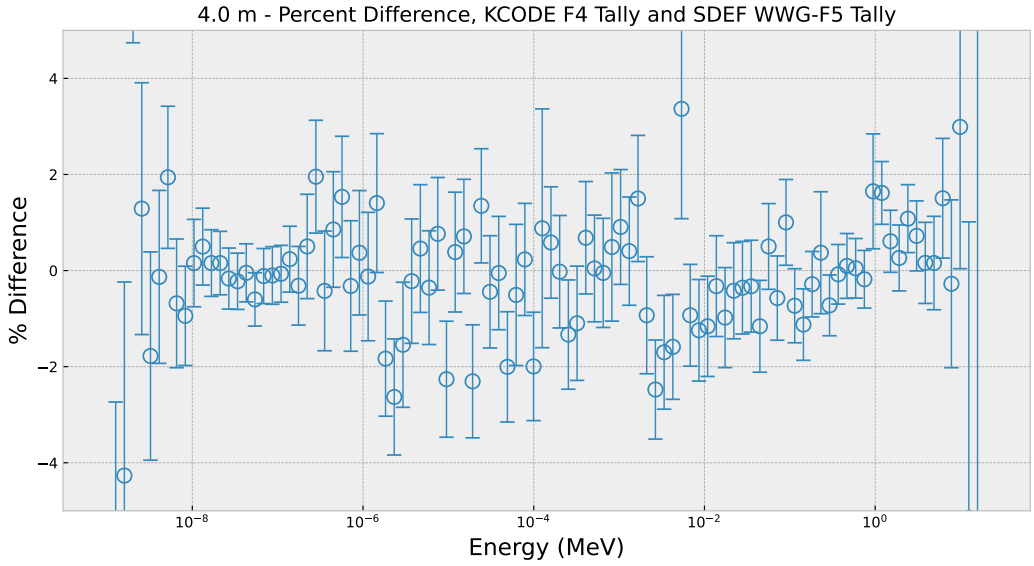

Figure 18: Percent Relative Difference in Neutron Energy Distribution, SDEF F5 WWG and KCODE F4

3 Conclusion

Significant progress was made to identify the major contributors to the large change in the neutron spectrum around Godiva following the assembly's move from LACEF to the DAF. The concrete room was confirmed to add the greatest contribution to the thermal energy peak observed by foil activation analysis. The plastic scintillator detectors and other large pieces of plastic also contribute to the spectrum, but their contribution is orders of magnitude lower. Following these findings, future modeling of the neutron energy spectrum around Godiva should continue to add fine detail for the concrete and plastic materials in the room to achieve the greatest accuracy.

The two variance techniques implemented showed good agreement with the standard KCODE implementation. Further efforts to understand best practices with variance reduction for the Godiva problem and for other critical assemblies is still needed. These preliminary results did show that the development of a framework for variance reduction for foil activation analysis will return significant improvement in the calculation speed. The F5 point detector tally reduced the runtime to 42739.55 minutes, and the WWG F5 method reduced the runtime to 1803.34 minutes. In future work, the DXTRAN variance reduction technique efficiency and ease of use will be assessed against these results.

References

[1] Rebecca S. Detwiler et al. *Compendium of Material Composition Data for Radiation Transport Modeling*. Tech. rep. PNNL-15870, Rev. 2. Richland, WA, USA: Pacific Northwest National Laboratory, 2021. DOI: 10.2172/1782721. URL: https://www.osti.gov/biblio/1782721.

[2] J.A. Favorite and J.M. Goda. "IER 555: Status of Godiva-IV Benchmark (HEU-MET-FAST-086) Revision". In: *Los Alamos National Laboratory* LA-UR-24-20990 (2024).

[3] Joetta Goda et al. "A New Era of Nuclear Criticality Experiments: The First 10 Years of Godiva IV Operations at NCERC". In: *Nuclear Science and Engineering* 195.sup1 (2021), S55–S79. DOI: 10.1080/00295639.2021.1947103.

[4] J.A. Kulesza et al. "MCNP Users Manual - Code Version 6.3". In: *Los Alamos National Laboratory* LA-UR-22-30006 (2022). See Section 1.2.5.